JOURNAL OF Materials CHEMISTRY

The preparation and characterisation of Langmuir–Blodgett films of the metal dithiolate charge-transfer complex *N*-octadecylpyridinium–Pd(dmit)$_2$

Christopher Pearson,[a] Zainol A. Ibrahim,[b] Ajaib S. Dhindsa,[c] Andrei S. Batsanov,[d] Martin R. Bryce,*[,d] Judith A. K. Howard,[d] Michael C. Petty*[,a] and Allan E. Underhill[c]

[a]*School of Engineering and Centre for Molecular Electronics, University of Durham, Durham, UK DH1 3LE*

[b]*Department of Physics, University of Malaya, 59100 Kuala Lumpur, Malaysia*

[c]*Institute of Molecular and Biomolecular Electronics, University of Wales, Dean Street, Bangor, Gwynedd, UK LL57 1UT*

[d]*Department of Chemistry and Centre for Molecular Electronics, University of Durham, Durham, UK DH1 3LE*

The behaviour of floating layers of *N*-octadecylpyridinium–Pd(dmit)$_2$, complex **1**, on the surface of a pure water subphase has been studied using pressure *versus* area isotherm measurements. Film properties were dependent on the quantity of material spread and the length of time that the layer was aged on the surface of the subphase before compression (spreading time). Area per complex values suggested that a monolayer was formed only if a small amount of material was applied to the subphase and the spreading time was long (several hours). Multilayer Langmuir–Blodgett (LB) films have been deposited onto hydrophilic glass substrates and examined using surface profiling, scanning electron microscopy with energy dispersive X-ray spectroscopy and optical absorption spectroscopy. Observations using electron microscopy showed that films deposited from fresh floating layers contained aggregates that were tens of microns in size. In contrast to previous studies on multilayer films of *N*-octadecylpyridinium–Ni(dmit)$_2$ complex, the LB films of complex **1** were electrically conductive without any post deposition doping treatment, with room temperature, in-plane conductivity values as high as 0.15 ± 0.10 S cm^{-1}. In some cases, super-Ohmic current *versus* voltage characteristics were recorded, which has been attributed to space-charge-limited conductivity. Multilayers transferred from aged floating layers did not exhibit significant bulk conductivity, either in the as-deposited state or after iodine doping, although some samples contained highly conductive crystallites that were several hundred microns in size. The single crystal X-ray structure of the analogous *N*-dodecylpyridinium–Pd(dmit)$_2$ complex is reported, which provides the first structural study of a [Pd(dmit)$_2$]$^-$ *mono*anion. The anions pack in centrosymmetric dimers, with an interplanar spacing of *ca.* 3.5 Å and Pd···S(5′) contacts of 3.57 Å, which are separated by *N*-dodecylpyridinium cations (with a Pd···N contact of 3.83 Å).

Over recent years, there has been growing interest in the preparation and characterisation of electrically conductive Langmuir–Blodgett (LB) films containing organic charge-transfer complexes.[1] Initial work concentrated on derivatives of molecules like the acceptor tetracyano-*p*-quinodimethane (TCNQ)[2] or the donor tetrathiafulvalene (TTF)[3] that had been modified to make them suitable for manipulation using the LB technique.[4] Multilayers containing these materials were semiconducting, with the most conductive films prepared having in-plane conductivity values in the range 10^{-2}–1 S cm^{-1} after chemical doping, which generated mixed valence species.

Systems containing molecules like TTF and TCNQ are characterised by strong one-dimensional interactions. In contrast, organometallic donor molecules such as metal(dmit)$_2$ (where metal = Ni, Pd, Pt, Au, and Zn and H$_2$dmit = 4,5-dimercapto-1,3-dithiole-2-thione) have peripheral sulfur atoms that can participate in both inter- and intra-stack interactions and hence increase the dimensionality of the system.[5] Japanese workers have investigated the electrical properties of LB films of a variety of metal(dmit)$_2$ complexes (metal = Ni, Pd, Pt, and Au) with long chain ammonium cations. Multilayer films of the complex tridecylmethylammonium–Au(dmit)$_2$ mixed with icosanoic acid to aid transfer and deposited by the horizontal lifting technique had room temperature conductivity values of around 10 S cm^{-1} after doping with bromine gas, and 25 S cm^{-1} after electrochemical oxidation in aqueous LiClO$_4$ solution.[6] Also, after electrochemical doping, metallic behaviour was observed between room temperature and 200 K.[6] Taylor *et al.* have prepared electrically conductive Y-type multilayer Langmuir–Blodgett films of a variety of metal–(dmit)$_2$ charge transfer salts (where metal = Au, Pd and Pt).[7] In some cases, a super-Ohmic current *versus* voltage characteristic was observed. This behaviour was attributed to space-charge-limited current flow.

We have previously characterised multilayer films containing Ni(dmit)$_2$ anions complexed with *N*-octadecylpyridinium (C$_{18}$Py). Langmuir–Blodgett films of the 2:1 complex (C$_{18}$Py)$_2$–Ni(dmit)$_2$ exhibited a stable in-plane conductivity with a maximum room temperature value after iodine doping of 0.8 S cm^{-1}.[8] Multilayer films of the 1:1 complex C$_{18}$Py–Ni(dmit)$_2$ have been used as the active region in an organic thin-film field effect transistor[9] and as a charge injection layer in an electroluminescent device.[10] The monolayer formation, multilayer deposition and LB film characterisation of this material have been extensively studied.[11] We now present a detailed study of the properties of the related 1:1 palladium complex, C$_{18}$Py–Pd(dmit)$_2$ (complex **1**), with particular emphasis on electrical characterisation of conducting LB layers. We also report the single crystal X-ray structure of the *N*-dodecylpyridinium–Pd(dmit)$_2$ analogue (complex **2**). The chemical structures of complexes **1** and **2** are shown in Fig. 1(*a*).

Experimental

Synthesis

The synthesis of complex **1** followed the reported procedure[7] for synthesis of the analogous 2:1 complex (C$_{18}$Py)$_2$–Pd(dmit)$_2$ with the important difference that the product was recrystal-

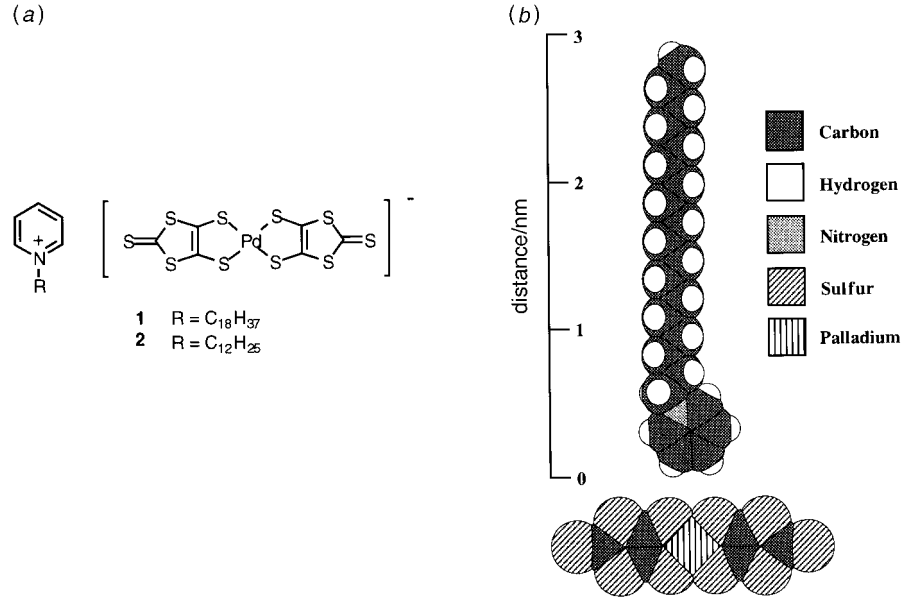

Fig. 1 (*a*) Chemical structures of complexes **1** and **2** and (*b*) space filling molecular model of complex **1**

lised from acetone in air (the air was required for oxidation) to produce the 1:1 complex as a very dark green solid. Elemental analysis: Found: C, 41.6; H, 5.1; S, 38.9%. $C_{29}H_{42}NPdS_{10}$ requires: C, 41.8; H, 5.1; S, 38.6%. A space filling model of complex **1** is shown in Fig. 1(*b*).

Complex **2** was synthesised in a similar manner, using *N*-dodecylpyridinium iodide, and isolated as very dark green–black crystals. Elemental analysis: Found: C, 37.4; H, 4.2; N, 1.9%. $C_{23}H_{30}NPdS_{10}$ requires: C, 37.0; H, 4.0; N, 1.9%.

Crystal structure determination

X-Ray diffraction experiments from a black plate-like crystal ($0.4 \times 0.12 \times 0.03$ mm) were performed at room temp. on a Siemens P4 four-circle diffractometer (graphite-monochromated Mo-Kα radiation, $\lambda = 0.71073$ Å). *Crystal data*: $C_{17}H_{30}N^+ C_6S_{10}Pd^-$(**2**): $M = 747.48$, triclinic, space group $P\bar{1}$ (No. 2), $a = 9.296(1)$, $b = 9.954(1)$, $c = 17.126(1)$ Å, $\alpha = 95.09(1)$, $\beta = 94.40(1)$, $\gamma = 99.99(1)^\circ$, $V = 1547.6(2)$ Å^3 (from 34 reflections, $9.3 < \theta < 12.0^\circ$), $Z = 2$, $D_c = 1.60$ g cm^{-3}, $F(000) = 762$, $\mu = 12.9$ cm^{-1}. Data collection: $\theta/2\theta$ scan mode, $2\theta \leqslant 50^\circ$, 6581 total data, 5448 unique data, $R_{int} = 0.068$. Analytical absorption correction (ABSPSI program,[12] $T_{min} = 0.856$, $T_{max} = 0.945$) gave only marginal improvement. The structure was solved by direct methods (SHELXS-86 programs[13]) and refined by full-matrix least-squares, using SHELXL-93 software,[14] against F^2 of all data with two-term weighting scheme (non-H atoms with anisotropic displacement parameters, all H atoms 'riding', total of 317 variables), converging at $R(F) = 0.048$ for 2817 'observed' data with $I \geqslant 2\sigma(I)$, $wR(F^2) = 0.116$ for all data, goodness-of-fit 0.814, residual $\Delta\rho_{max} = 0.73$, $\Delta\rho_{min} = -0.69$ e Å^{-3}. Full crystallographic details, excluding structure factors, have been deposited at the Cambridge Crystallographic Data Centre; see Information for Authors, *J. Mater. Chem.*, 1998, Issue No. 1. Any request to the CCDC for this material should quote the full literature citation and the reference number 1145/64.

Monolayer formation

Surface pressure *versus* area per complex measurements and LB deposition were undertaken in a class 10 000 microelectronics clean room using constant perimeter barrier troughs that were designed and built in Durham.[15] Complex **1** could be deposited in pure form but the solid was only slightly soluble in chloroform, so a mixed solvent consisting of dichloromethane–benzene in the volume ratio 3:2 was used. To prepare a solution, 3 ml of dichloromethane was added to *ca.* 1 mg of solid material in a volumetric flask. The mixture was agitated in an ultrasonic bath for 10 min before 2 ml of benzene was added to give a final concentration of *ca.* 0.2 g l^{-1}. A pure water subphase (obtained by reverse osmosis, deionisation and ultraviolet sterilisation) at a pH of 5.8 ± 0.2 and a temperature of 20 ± 2 °C was used, and a suitable volume of solution (0.5–3 ml) was distributed over the surface of this using a microsyringe. The floating layer was left uncompressed for between 1 min and 21 h. Pressure *versus* area isotherms were plotted at a compression speed of $(2.3 \pm 1.7) \times 10^{-3}$ nm^2 complex^{-1} s^{-1}.

Multilayer LB film characterisation

Multilayer LB structures were built up on hydrophilic glass slides. These were cleaned by scrubbing with Decon 90 (Decon Laboratories Limited) using a polishing pad, ultrasonic agitation in a 5% solution of Decon 90 for 30 min, rinsing with ultrapure water, ultrasonic agitation in ultrapure water for 30 min, and finally drying in a stream of nitrogen gas. Film thicknesses were measured using a Tencor Instruments Alpha-Step 200 surface profilometer, with a stylus force of 11 ± 1 mg. For these measurements, a step was created by wiping away a portion of the film with a tissue soaked in dichloromethane. A layer of aluminium approximately 150 nm thick was then evaporated over this step to prevent the stylus of the instrument from penetrating the surface of the organic film. Film morphology was investigated using a Vickers optical microscope and a Cambridge Instruments Stereoscan 600 scanning electron microscope, operating at 15 kV, together with a Link Systems 860 Series 2 energy dispersive X-ray spectrometer (EDS). Optical absorption spectra were recorded using a Perkin-Elmer Lambda 19 UV–VIS–NIR spectrophotometer with a resolution of 1 nm.

Films were doped by exposure to crystals of iodine in a sealed container. The in-plane dc conductivity was measured using a two probe technique. Electrical contacts, 5.0 ± 0.5 mm long and between 1.0 ± 0.5 and 5.0 ± 0.5 mm apart, were made using carbon cement (Neubauer Chemikalien). A Time Instruments 2003S voltage calibrator was the voltage source and the current was measured using a Keithley 414A picoammeter. Room temperature measurements were performed in a screened metal sample chamber which, if required, could be evacuated to a pressure of *ca.* 10^{-2} m bar using a rotary pump. Low temperature data, within the range 77–300 K, were obtained under a low pressure of helium in an Oxford Instruments DN704 exchange gas cryostat.

Results

Behaviour of floating films

Reproducible isotherms and LB deposition were obtained for complex **1**, but not for complex **2**, which suggests that the longer alkyl chain is a prerequisite for good quality film formation in this series of compounds. The studies reported below are, therefore, restricted to compound **1**. Condensed surface pressure *versus* area isotherms were recorded, but the shape of the plot was found to have a strong dependence on the time that the layer was left on the surface of the subphase before compression (spreading time), as well as on the amount of solution spread. In Fig. 2(*a*), examples of isotherms recorded at different times after the application of 1 ml of a solution of compound **1** to the surface of the subphase are shown. After a spreading time of 1 min, the area per complex, measured at a surface pressure of 30 mN m^{-1}, was *ca.* 0.12 nm^2, and a plateau region was evident in the plot. This was thought to be associated with reorganisation of the floating layer. A significant increase in the area per complex was observed if the floating film was left uncompressed for longer times. After 10 min, for example, the area per complex at 30 mN m^{-1} was *ca.* 0.26 nm^2, increasing to *ca.* 0.36 nm^2 after 18 h. Also, for longer times, the plateau region disappeared from the curve. Similar results have been obtained from the pressure *versus* area isotherms of floating layers of C_{18}Py–Ni(dmit)$_2$.[11] Here, the area per complex at 30 mN m^{-1} increased from 0.05 to 0.25 nm^2 when the spreading time was increased from 5 min to 3 h, and a maximum value of 0.30 nm^2 was reached after a spreading time of approximately 5 h. Taylor *et al.* have also observed comparable behaviour in the isotherms of the 2:1 salts bis(didodecyldimethylammonium)–metal(dmit)$_2$ (metal = Ni,[16] Pd and Pt).[17] Changes in the isotherms of these complexes were observed, with the area per complex moving to higher values, as the spreading time was increased.

Fig. 2(*b*) contrasts isotherms recorded 10 min after the spreading of 1 ml and 2 ml of a solution of complex **1**. When a large volume of solution was spread, a small area per complex at 30 mN m^{-1} of *ca.* 0.15 nm^2 was observed, with a plateau at *ca.* 27 mN m^{-1}. When the volume of solution spread was reduced to 1 ml, spreading was improved, and an increased area per complex of *ca.* 0.26 nm^2 at 30 mN m^{-1} was recorded. A similar trend was observed in work with floating films of C_{18}Py–Ni(dmit)$_2$, where the area per complex at 30 mN m^{-1}, after a spreading time of 15 min, was seen to decrease from 0.085 to 0.035 nm^2 when the volume of spreading solution was increased from 1 to 5 ml.[11] Gupta *et al.*[17] also observed similar behaviour in their divalent metal(dmit)$_2$ salts with didodecyldimethylammonium cations. They found that increasing the amount of material applied to the surface of the subphase shifted the isotherm to lower areas, and implied that this was due to poor spreading of the complexes. Fig. 3 is a plot of area per complex, measured at a surface pressure of 30 mN m^{-1}, *versus* the time that uncompressed films of complex **1** were aged on the subphase surface. Data obtained for various different volumes of spreading solution are plotted on the same graph. It is evident that for short times, aggregation or multilayer formation occurred, and the area per complex was correspondingly small. After extended times, the molecules rearranged, and the area occupied by each complex increased. Gupta *et al.*[17] have used microscopy to examine LB multilayers of the monovalent salt didodecyldimethylammonium –Ni(dmit)$_2$. A nine-layer film deposited after a spreading time of 20 min was composed of a mass of microcrystallites. After a spreading time of 1 h, the number of microcrystallites contained in another nine-layer film was significantly reduced.

From space filling molecular models, the dimensions of the *N*-octadecylpyridinium cation were found to be $0.8\pm0.1\times0.3\pm0.1\times2.9\pm0.1$ nm and those of the Pd(dmit)$_2$ molecule were $1.6\pm0.1\times0.6\pm0.1\times0.4\pm0.1$ nm. These data are supported by the single crystal X-ray study of the *N*-dodecylpyridinium complex **2** discussed below. The maximum area per complex measured here, *i.e. ca.* 0.33 nm^2, when a small amount of solution was spread and allowed to stand uncompressed for a long time, was lower than that expected for a film in which both components were in contact with the subphase, *i.e.* 0.24 nm^2 for the *N*-octadecylpyridinium cation and a minimum of 0.24 nm^2 for the Pd(dmit)$_2$ molecule, giving a total of 0.48 nm^2. Similar behaviour was observed for floating films of C_{18}Py–Ni(dmit)$_2$. A possible arrangement of the molecules in these films has been proposed,[11] with the Ni(dmit)$_2$ anions interdigitated between the alkylpyridinium cations which are tilted at an angle of *ca.* 30° to the substrate

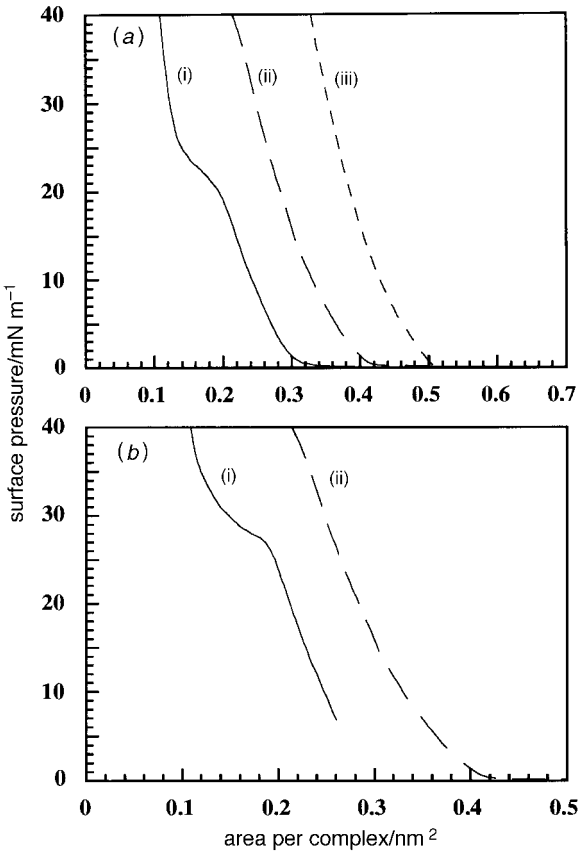

Fig. 2 Surface pressure *versus* area isotherm plots for floating films of complex **1** (*a*) (i) 1 and (ii) 10 min and (iii) 18 h after the spreading of 1 ml of solution on a pure water subphase, and (*b*) 10 min after the spreading of (i) 1 and (ii) 2 ml of solution on a pure water subphase

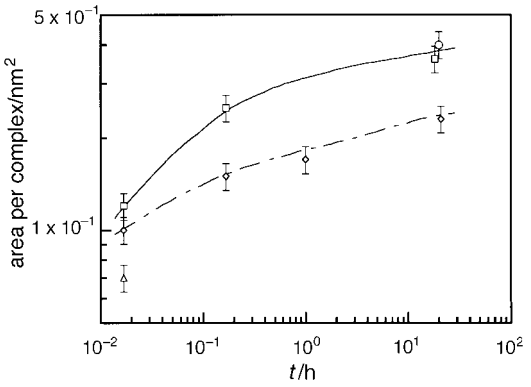

Fig. 3 Area per complex, measured at a surface pressure of 30 mN m^{-1}, *versus* the time that molecules of complex **1** were allowed to remain on the surface of a pure water subphase before isotherms were recorded: (○) 0.5, (□) 1, (◇) 2 and (△) 3 ml

normal. We suggest a similar arrangement for the molecules in layers of $C_{18}Py–Pd(dmit)_2$. An area per complex of around 0.3 ± 0.1 nm^2 would be expected for this structure, close to the maximum value recorded for floating films of complex **1**. Polarised IR spectroscopy would be necessary to provide further evidence for this structure.

A comparison of isotherms recorded after long spreading times revealed that if the amount of solution applied to the subphase was increased, the area per complex value decreased. Observation of floating layers formed from a large volume of solution after a long spreading time revealed the existence of aggregates at the air–water interface. Using atomic force microscopy, Yamura *et al*. have observed micron sized, plate-like crystallites present in monolayer and multilayer LB films of tridecylmethylammonium–$Au(dmit)_2$ mixed with icosanoic acid.[18] It was thought that these platelets formed at the air–water interface and were subsequently transferred to the substrate during monolayer transfer. This was consistent with the small area per molecule that had been obtained from surface pressure *versus* area measurements.[19]

LB deposition

In experiments where an isotherm with no plateau was recorded, a deposition pressure of 30 mN m^{-1} was used. When a plateau was observed, a surface pressure of 38 mN m^{-1} (above the plateau) was substituted. Dipping was started with the substrates in air above the surface of the subphase and was undertaken at a speed of 6 mm min^{-1}, allowing 15 min of drying time between cycles. The substrates used were hydrophilic glass slides, and consequently the first cycle exhibited Z-type transfer. Subsequently, transfer was Y-type, with a transfer ratio that was dependent on the exact spreading conditions. A maximum value of 1.1 ± 0.1 was recorded when the floating layer was formed from 2 ml of solution, regardless of the spreading time.

Film thickness

A typical surface profiling scan, obtained from a 19-layer film that had been transferred from a floating layer formed from 1 ml of solution compressed after 10 min on the subphase, is shown in Fig. 4. The film was continuous up to a thickness of *ca*. 90 nm, but the surface was undulating, and a number of regions up to 200 nm thick and 50 μm in diameter were recorded, as well as a 'giant' peak close to the edge of the film. The latter was attributed to physical damage caused as the step was formed by wiping away a portion of the film, resulting in an accumulation of organic material at the edge of the step. The results of four experiments are listed in Table 1. The best spreading characteristics, and hence the thinnest layers, were observed when 1 ml of solution was spread and the film left on the subphase for 18 h before compression. The values obtained here for the area per complex and thickness per layer suggest that a monolayer may be formed under these conditions. Thicker layers were deposited if the film was compressed earlier or if more solution was spread, indicating aggregation or the formation of multilayer films at the air–water interface.

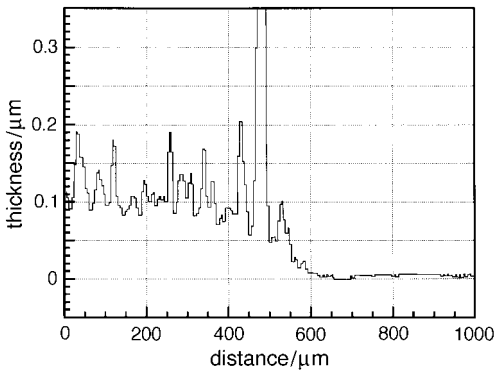

Fig. 4 A typical surface profiling Alpha-Step trace, recorded from a 19-layer film of complex **1**. The sample was deposited from a floating layer formed from 1 ml of solution that had been allowed to stand on the surface of the subphase for 10 min before compression. The sample was overcoated with a layer of aluminium *ca*. 150 nm thick to prevent the stylus from penetrating the surface of the organic film.

Table 1 The variation in layer thickness with the volume of solution of complex **1** that was spread and the length of time allowed before compression

volume of solution spread/ml	time before compression	thickness per layer/nm
1	10 min	4.7 ± 0.2
1	18 h	2.5 ± 0.3
2	10 min	11.4 ± 0.2
2	21 h	5.7 ± 0.3

Scanning electron microscopy

Fig. 5(*a*) shows a scanning electron micrograph obtained from a 19-layer film deposited onto a glass substrate from a film formed from 1 ml of solution that had been allowed to stand on the subphase uncompressed for 10 min. Irregularly shaped

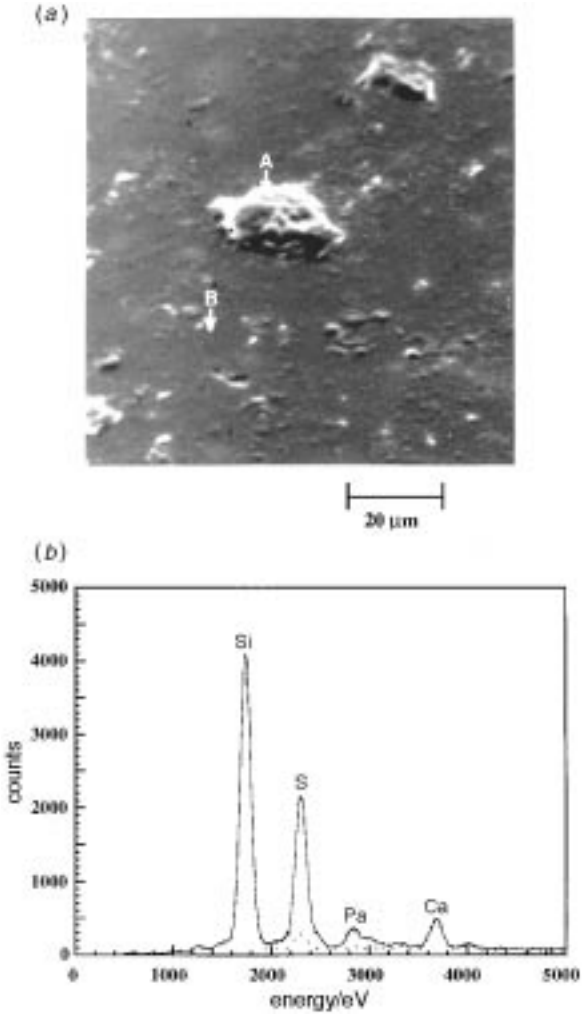

Fig. 5 (*a*) Scanning electron micrograph of an as-deposited 19-layer film of complex **1**. The sample was transferred from a layer formed from 1 ml of solution that had been allowed to stand on the surface of the subphase for 10 min before compression. (*b*) EDS spectra recorded from the same film. The electron probe was directed at point A on the micrograph shown in (*a*) when the solid line was recorded and at point B for the data represented by the dashed line.

aggregates can be seen, tens of microns in size, *i.e.* having similar dimensions to the thick regions seen in previous surface profiling scans (Fig. 4). Fig. 5(*b*) shows the results of EDS measurements for the two electron probe positions marked on the micrograph, corresponding to one of the aggregates (position A) and the background (position B). Sulfur and palladium were predominantly detected when the aggregate was probed, although traces of these elements were also seen in the background spectrum, indicating the presence of $Pd(dmit)_2$. Using this technique it was not possible to detect the presence of the long chain pyridinium cations. The strong signals due to silicon and calcium were due to the substrate, confirmed by an EDS measurement on an uncoated piece of glass. When the same amount of solution was spread but 18 h allowed before compression, no large aggregates were found. It is therefore suggested that when 1 ml of solution was spread, large crystallites containing $Pd(dmit)_2$ were immediately formed. These crystallites dissociated with time on the surface of the subphase giving a more uniform floating film, similar to observations for films of didodecyldimethylammonium–$Ni(dmit)_2$.[17b]

When 2 ml of solution was spread and compressed after 10 min on the subphase, a higher density of crystallites was observed [Fig. 6(*a*), from a 19-layer as-deposited film]. After ageing, much larger aggregates formed which were hundreds of microns in size. These clusters could be observed in the layer on the surface of the subphase and were subsequently transferred to the substrate. A micrograph recorded from a 39-layer sample deposited from a film formed from 2 ml of solution that had been allowed to stand uncompressed for 21 h is shown in Fig. 6(*b*), where one of the large particles can clearly be seen. EDS scans were performed with the electron probe directed first at the aggregate (position A) and then at the background (position B). Large signals due to sulfur and palladium were observed when the crystallite was probed, revealing the presence of $Pd(dmit)_2$. When the background was examined, however, the peaks due to these elements were much lower. Signals originating from the silicon and calcium in the glass substrate were once again recorded.

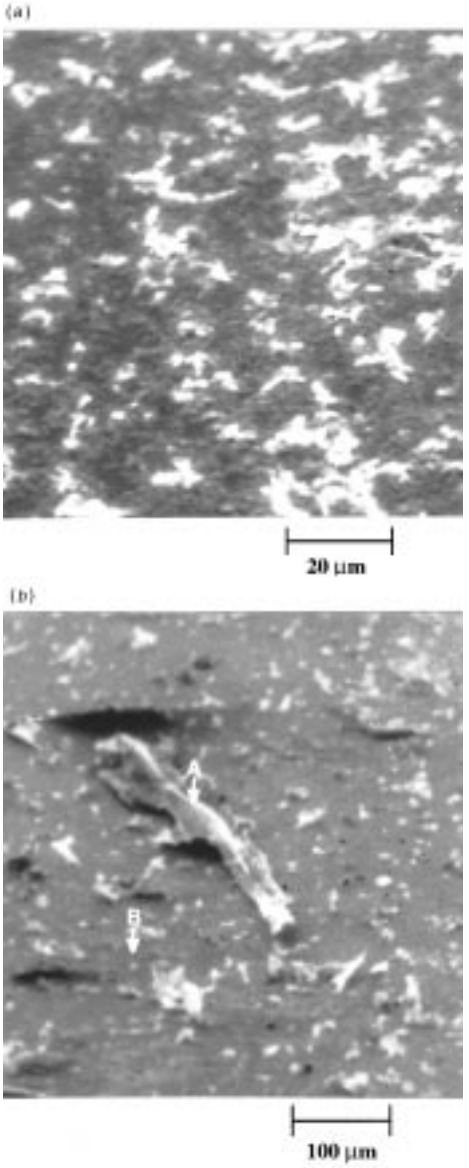

Fig. 6 Scanning electron micrographs of as-deposited films of complex **1**. (*a*) A 19-layer sample transferred from a floating film formed from 2 ml of solution that had been allowed to stand on the surface of the subphase for 10 min before compression and (*b*) a 39-layer sample transferred from a floating film formed from 2 ml of solution that had been allowed to stand on the surface of the subphase for 21 h before compression, showing aggregate (position A) and background (position B).

Optical absorption

The optical absorption spectra for as-deposited films of complex **1** transferred from floating layers formed from different amounts of solution that had been left on the subphase for different times are shown in Fig. 7(*a*). The figure includes spectra obtained from four samples as detailed in the caption. The absorption bands that were observed at 330, 380 and 480 nm are probably due to intramolecular transitions within the $Pd(dmit)_2$ molecules. Additionally, for electrically conductive films, broad bands were seen at 800 and 1400 nm. Absorptions in the near infrared have been associated with intermolecular charge-transfer transitions by Underhill *et al.*[19] in single crystals of $Cs[Pd(dmit)_2]_2$ and Miura *et al.* for LB multilayers of tridecylmethylammonium–$Au(dmit)_2$ mixed with icosanoic acid and deposited by the horizontal lifting method.[20] The variation in the intensity of the absorption bands reflects the different film thicknesses obtained under different spreading conditions, and a plot of absorption, measured at 800 nm, *versus* film thickness, measured using surface profiling, is shown inset to Fig. 7(*a*). The graph indicates an approximately linear relationship between the two quantities.

Spectra recorded for the same films after chemical doping are shown in Fig. 7(*b*). After treatment with iodine vapour, the bands at 380 and 480 nm and the broad absorption in the infrared were significantly reduced, whereas the band at *ca.* 800 nm remained. Two peaks were observed, at a similar wavelength, in the spectra of conductive iodine-doped films of $C_{18}Py$–$Ni(dmit)_2$.[11] It seems likely that some (or all) of these absorptions are associated with a charge-transfer band arising from the existence of a mixed valence complex.

In-plane electrical conductivity

The current *versus* voltage characteristics for a 19-layer film of complex **1** deposited from a layer formed from 1 ml of solution that had remained uncompressed on the subphase for 10 min are shown in Fig. 8. Measurements were performed under vacuum, using carbon cement contacts with different spacings. The film was found to be conducting without the need for any post-deposition doping treatment. This behaviour is consistent with the presence of bands in the near infrared at *ca.* 800 and 1400 nm in the optical absorption spectrum of the film. A band at 800 nm has been attributed to an intermolecular charge transfer transition in single crystals of $Cs[Pd(dmit)_2]_z$.[19] Using the thickness of the film obtained from surface profiling measurements, a room temp., in-plane dc conductivity of $3.5 \pm 2.5 \times 10^{-3}$ S cm^{-1} at a bias of 1 V was calculated. This value is much higher than that measured for as-deposited films of $C_{18}Py$–$Ni(dmit)_2$.[11] The bulk sample of complex **1** was non-conductive ($\sigma_{rt} = < 10^{-8}$ S cm^{-1}, two-

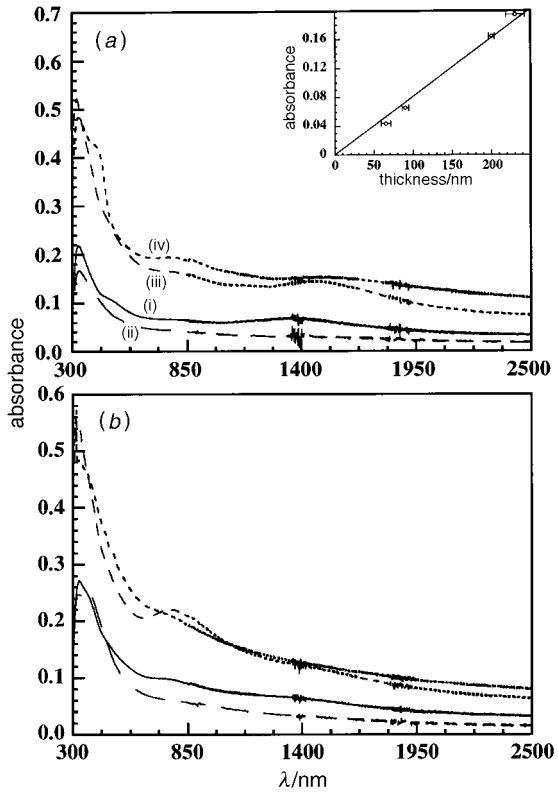

Fig. 7 Optical absorption spectra for multilayer LB films of complex **1** prepared from floating layers formed from different amounts of spreading solution that had been allowed to age on the subphase for different lengths of time (*a*) as-deposited (the absorbance at 800 nm *versus* measured film thickness is shown inset, error bars are derived from six scans) and (*b*) after iodine doping: (i) 1 ml, 10 min, 19 layers; (ii) 1 ml, 18 h, 19 layers; (iii) 2 ml, 10 min, 19 layers; (iv) 2 ml, 21 h, 39 layers

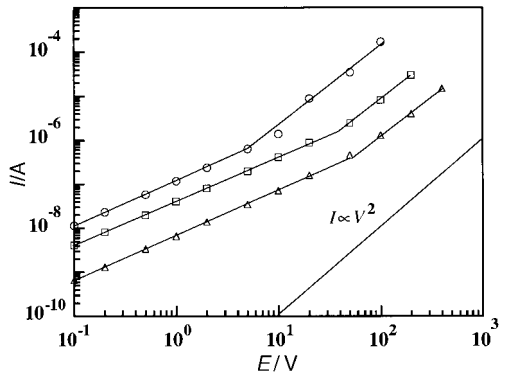

Fig. 8 Room temperature in-plane current *versus* voltage characteristics for an as-deposited 19-layer LB film of complex **1** with contacts (○) 1, (□) 3 and (△) 5 mm apart. The sample was transferred from a floating layer formed from 1 ml of solution that had been allowed to stand uncompressed on the surface of the subphase for 10 min.

probe, compressed pellet measurement). The reason for this high conductivity in LB films of **1** without any post-deposition doping is not understood. However, a relatively high conductivity of 10^{-2} S cm^{-1} has been previously reported[21] for LB films of the 1:1 salt *N*-octadecylpyridinium–TCNQ. It was suggested that inadvertent doping with anions (such as OH^-) during the deposition procedure may have been responsible.

The current *versus* voltage characteristics for as-deposited C_{18}Py–Ni(dmit)$_2$ was not a simple straight-line relationship over the entire voltage range studied, and a super-Ohmic region was observed at high bias.[11] In this region, current saturation was slow, and a few tens of minutes were required for the current to reach its peak value. Under high bias, the peak sample current was found to be proportional to the square of the applied voltage. Taylor *et al.*[7] have observed super-Ohmic current *versus* voltage behaviour in films of bis(didodecyldimethylammonium)–Pt(dmit)$_2$, bis(octadecylpyridinium)–Pd(dmit)$_2$ and octadecylpyridinium–Au(dmit)$_2$ with evaporated gold contacts, and the same effect was seen in multilayers of the 2:1 complex (*N*-octadecylpyridinium)$_2$–Ni(dmit)$_2$.[8b] This behaviour may indicate space-charge-limited conductivity (SCLC),[22] which is described by the general law shown in eqn. (1),

$$J \propto L\left(\frac{V}{L^2}\right)^n \tag{1}$$

where J is the current density, V the bias voltage, L the thickness of the sample and n is a constant. For single carrier injection (electrons or holes), $n=2$. A graph of sample current at a bias of 100 V *versus* the distance (on a log *versus* log scale) between contacts, L, for complex **1** is shown in Fig. 9. The best fit to these data, represented by the dashed line, has a slope of -2.9 ± 0.2. Hence, eqn. (1) is satisfied with $n=2$. From the same model, the threshold voltage $V_{\Omega c}$, where the Ohmic current crosses over into the SCL regime is given by eqn. (2),

$$V_{\Omega c}=\frac{8}{9}\frac{enL^2}{\varepsilon\theta_n} \tag{2}$$

where e is the electronic charge, n is the concentration of conduction electrons, ε is the permittivity and θ_n the fraction of total carriers that are free. From this equation, it can be seen that for SCLC, $V_{\Omega c}$ should be proportional to the square of the thickness of the sample. By fitting straight lines to the Ohmic and super-Ohmic portions of the experimental current *versus* voltage characteristics, this threshold voltage has been obtained for the different distances between contacts, L. A plot of $\sqrt{V_{\Omega c}}$ *versus* L is shown in Fig. 10. The points lie on a

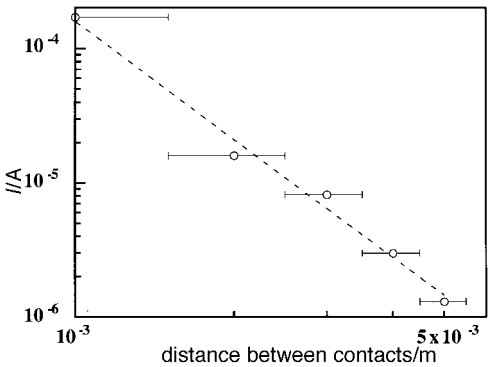

Fig. 9 Current, at a bias of 100 V, *versus* the distance between contacts on an as-deposited 19-layer LB film of complex **1**. The dashed line represents the best fit to the data, and has a slope of -2.9 ± 0.2.

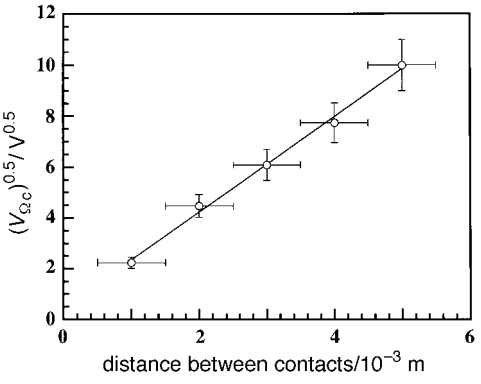

Fig. 10 A plot of $(V_{\Omega c})^{0.5}$ *versus* the distance between contacts on a 19-layer as-deposited film of complex **1**. The film was transferred from a floating layer prepared from 1 ml of solution and compressed 10 min after spreading. (All data were obtained from the same sample.)

straight line, in agreement with eqn. (2). These results strongly suggest that the observed super-Ohmic characteristics are caused by single carrier space-charge injection.

High conductivity was retained after the removal of bias in the SCLC region. It is possible for the accumulation of charge to affect current readings in materials where SCLC is observed.[23] Fig. 11 shows the variation of the conductivity of a 19-layer film of complex **1**, with carbon cement contacts 2.5 ± 0.5 mm apart, as the voltage was cycled from 10^{-1} to 5×10^2 V and back again. The conductivity increased with increasing bias, and the high value was retained as the voltage was reduced again. This high conductivity remained for a considerable time after the removal of bias in the SCLC regime. For example, Fig. 12 shows the variation of current with time when a bias of 10 V was applied to carbon cement contacts, 1.0 ± 0.5 mm apart on a 19-layer LB sample, after a voltage of 100 V, in the SCLC region, had previously been applied until current saturation occurred. The conductivity returned to a level close to the value recorded before the application of high bias only after several months. It is also possible that the applied electric field is in some way leading to a better organisation of the molecules in the film which could result in a higher conductivity, *i.e.* a poling process. Subsequently, the film could become more disordered with time.

After doping with iodine, the super-Ohmic region in the current *versus* voltage characteristic was seen to disappear. From room temperature measurements, a high conductivity of $2.6 \pm 1.7 \times 10^{-2}$ S cm^{-1} was calculated. The conductivity value

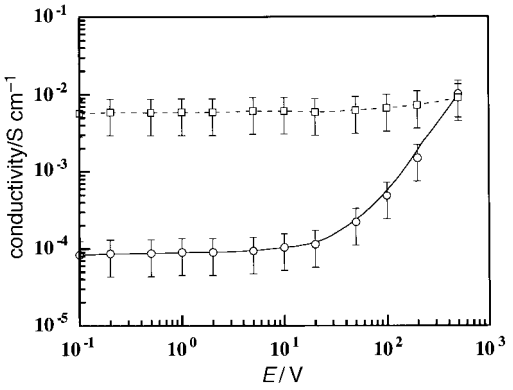

Fig. 11 The variation of the conductivity of a 19-layer as-deposited film of complex **1** with bias voltage. The film was deposited from a floating layer formed from 1 ml of solution that was aged for 10 min before compression (the contacts were 1.0 ± 0.5 mm apart): (○) bias increasing and (□) bias decreasing

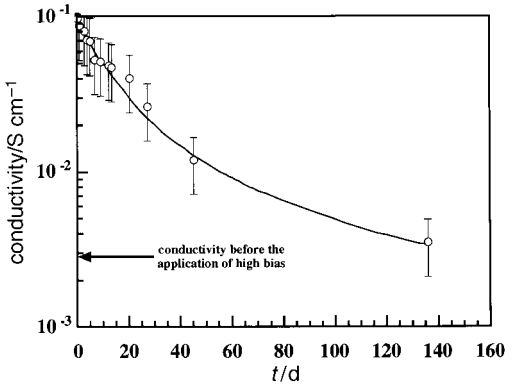

Fig. 12 Variation of the conductivity with time (with a bias of 10 V applied to carbon cement contacts 1.0 ± 5 mm apart) of a 19-layer as-deposited film of C_{18}Py–Pd(dmit)$_2$. The film was transferred from a floating layer formed from 1 ml of solution aged for 10 min before compression. The sample was pre-treated by the application of 100 V until current saturation occurred.

was higher than that measured for the as-deposited sample which was transferred from a floating layer prepared under the same spreading conditions, but lower than those obtained for multilayer films of C_{18}Py–Ni(dmit)$_2$[11] and (C_{18}Py)$_2$–Ni(dmit)$_2$[8b] after iodine doping. The high conductivity values for films of complex **1** are consistent with the results of optical absorption experiments. In Fig. 7, the spectra recorded for these films are similar before and after doping, with bands at 800 and 1400 nm.

Multilayer samples of complex **1** deposited from floating films formed from 1 ml of solution that was allowed to age on the subphase for 18 h were non-conductive ($\sigma < 10^{-8}$ S cm^{-1}) in the as-deposited state (in agreement with data for the bulk sample given above). After exposure to iodine vapour the conductivity of complex **1** was seen to rise to 10^{-5}–10^{-4} S cm^{-1} initially, but rapidly to fall back to the as-deposited value on application of vacuum. The optical absorption spectra for these films (as-deposited and after iodine doping and vacuum treatment) exhibited no bands in the near infrared, consistent with the lack of conductivity. Our previous model for LB multilayers deposited from aged floating films of C_{18}Py–Ni(dmit)$_2$ offers an explanation for these observations.[11] In this structure, the metal(dmit)$_2$ molecules (metal = Pd and Ni) are prevented from packing closely in either direction. This would effectively prevent charge-transfer (with characteristic optical absorption bands in the near infrared) and prohibit high in-plane conductivity. The proposed molecular arrangement is similar to that suggested by Taylor *et al.*[24] for floating layers of 1:1 and 2:1 salts of didodecyldimethylammonium and Ni(dmit)$_2$, based on the measurement of limiting area per complex values. Here, the close packed cations were interspersed with vertically stacked anions with their long axes either parallel or perpendicular to the surface of the subphase.

When multilayer samples of complex **1** were prepared from a floating layer formed from 2 ml of solution that had been allowed to stand on the surface of the subphase for 10 min before compression, high conductivity was once again observed without any post deposition doping (consistent with the presence of bands in the near infra-red absorption spectrum). The current *versus* voltage behaviour of an as-deposited 17-layer film, with contacts that were 1.0 ± 0.5 mm apart, was Ohmic over most of the bias range studied, with a slight departure from linear behaviour seen only at the upper voltage limit. A conductivity of $1.5 \pm 1.0 \times 10^{-1}$ S cm^{-1} was calculated from this characteristic, which is similar to that of C_{18}Py–Ni(dmit)$_2$ films after iodine doping.[10] After chemical doping of the same 17-layer film of complex **1** with iodine, the behaviour was again predominantly Ohmic. The conductivity was similar after doping, with a value of $6.0 \pm 4.0 \times 10^{-2}$ S cm^{-1}.

In common with multilayer samples transferred from 1 ml of solution that had been aged before compression, films deposited from floating layers formed from 2 ml of solution that had been allowed to stand uncompressed on the subphase for 21 h had bulk conductivity that was too low to measure, either in the as-deposited state or after doping with iodine. Visible crystallites were present in these films, however, and by carefully making contact to these with carbon cement, and recording a current *versus* voltage characteristic, these were found to be electrically conductive. Fig. 13(*a*) is an electron micrograph of one such conductive aggregate contained in a 39-layer film. The contacts to the cluster can be seen as dark areas at the sides of the micrograph. Fig. 13(*b*) is a surface profiling scan taken across the aggregate, along the line indicated by the arrow on Fig. 13(*a*). The scan reveals that the feature is ~ 500 μm long and 1–2 μm thick. Conductivity values (calculated from current *versus* voltage characteristics and using the dimensions of the crystallite measured from the micrograph and the surface profiling scan) of $1.2 \pm 1.0 \times 10^{-1}$ and $4.0 \pm 3.3 \times 10^{-2}$ S cm^{-1} were obtained, before and after doping, respectively. These values are similar to those obtained

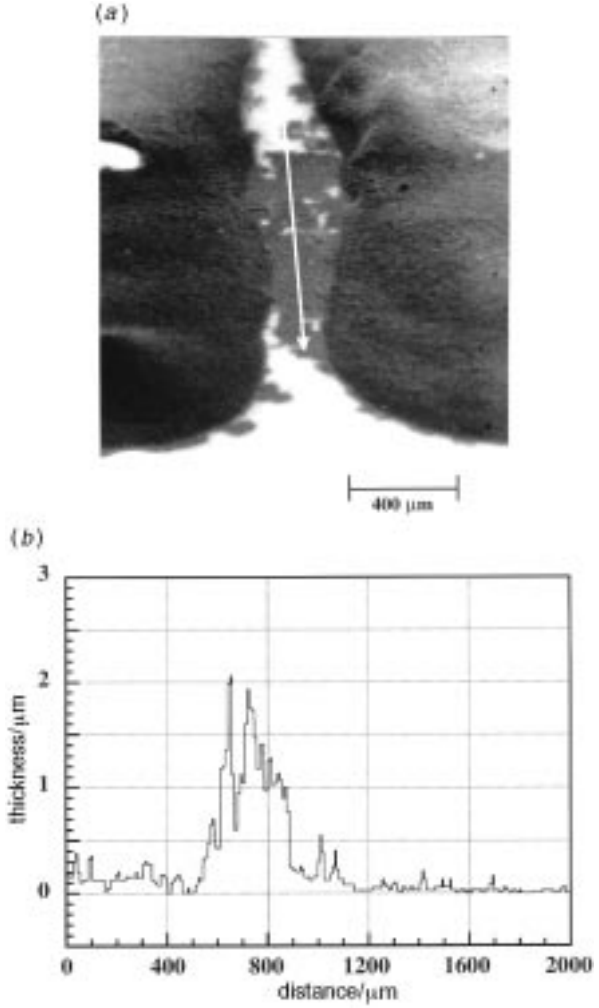

Fig. 13 (*a*) A scanning electron micrograph of a visible aggregate contained in a 39-layer LB film of complex **1**. The dark regions at the sides of the micrograph are carbon cement contacts. The arrow indicates the direction of the surface profiling scan used to obtain the trace shown in (*b*). (*b*) A surface profiling Alpha-Step scan of the aggregate shown in (*a*) The film containing the crystallite was transferred from a floating layer formed from 2 ml of solution that was aged for 21 h before compression.

for the bulk conductivity of multilayer samples deposited from films formed from 2 ml of solution compressed after 10 min floating on the surface of the subphase.

Low temperature conductivity

Two semi-logarithmic current *versus* reciprocal temperature plots recorded for a 19-layer sample of complex **1** prepared from a film formed from 1 ml of solution allowed to stand on the subphase for 10 min before compression are shown in Fig. 14(*a*). The current *versus* voltage characteristics at the extremes of temperature are shown inset. To make the current measurements, bias voltages of 1 and 200 V (in the linear and super-Ohmic parts of the current *versus* voltage characteristics) were applied. These data deviate from the simple straight line relationship predicted by eqn. (3),

$$\sigma = A \exp\left(-\frac{\Delta E}{kT}\right) \quad (3)$$

where A is a constant, and ΔE is the thermal activation energy. The temperature dependence of the electrical conductivity of a semiconductor involves the contributions due to (*a*) changes in carrier concentration, from (*i*) thermal activation and (*ii*) the density of states in the transport band, which varies as $T^{3/2}$, and (*b*) fluctuating carrier mobility, μ, (due to scattering),

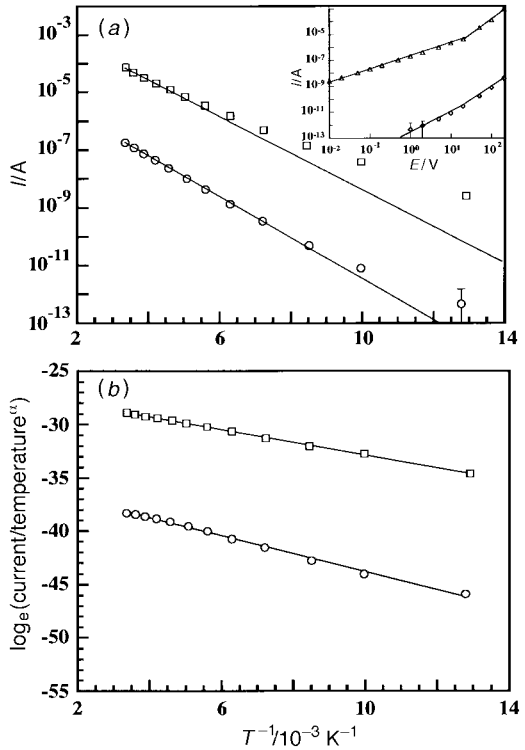

Fig. 14 (*a*) Semi-logarithmic plots of current [with bias voltages of (○) 1 and (□) 200 V] *versus* reciprocal temperature for a 19-layer as-deposited LB sample of complex **1** deposited from a floating layer formed from 1 ml of solution that was aged on the subphase for 10 min before compression. The current *versus* voltage characteristics at the extremes of the temperature range studied are shown inset: (◇) 78.2 and (△) 297.4 K. (*b*) The current *versus* reciprocal temperature data of (*a*) corrected for the effect of a temperature-dependent carrier mobility: $\alpha = 4.0$ for bias of 1 V; $\alpha = 3.4$ for bias of 200 V.

which typically varies as T^n with $-3 \leqslant n \leqslant 3/2$. If the temperature dependence of the mobility is dominated by lattice scattering, then $\mu \propto T^{-3/2}$, and a weak temperature dependence would be expected from the product of mobility and density of states. If, however, mobility is controlled by impurity scattering, $\mu \propto T^{3/2}$, and the product of mobility and state density has a T^3 dependence. Epstein *et al.*[25] have used an equation of the form eqn. (4),

$$\sigma = \sigma_0\, T^{\alpha} \exp\left(-\frac{\Delta}{T}\right) \quad (4)$$

where $\Delta = \Delta E/k$, to describe the temperature dependence of the conductivity of some organic single crystals (such as NMP–TCNQ) (NMP = *N*-methylphenazinium) where there is a thermally activated carrier concentration, $n \propto \exp(-\Delta/T)$ and a temperature dependent mobility, $\mu \propto T^{\alpha}$. They measured α values in the range -3 to -4 for a range of TCNQ systems, attributed to the interaction of charge carriers with molecular vibrations. In this situation, a graph of $\log_e(I/T^{\alpha})$ *versus* $1/T$ would be expected to yield a straight line. Good linear fits to the experimental data for the LB films of complex **1**, at bias voltages of 1 and 200 V were obtained when $\log_e(I/T^{\alpha})$ *versus* $1/T$ was plotted with $\alpha = 4.0$ and 3.4, respectively, as shown in Fig. 15(*b*). This suggests a power law temperature dependence of conductivity, with contributions from the state density and a carrier mobility variation dominated by impurity scattering. Activation energies that were the same within the limits of the experimental error, *i.e.* 0.07 ± 0.01 and 0.05 ± 0.01 eV, were calculated from the slopes of these graphs for low and high bias voltages, respectively. Nakamura *et al.*[26] have measured a similar activation energy of 0.065 eV for LB films of didecyldimethylammonium–Ni(dmit)$_2$, and Miura *et al.*[27] have reported a value of 0.05 eV for LB films of

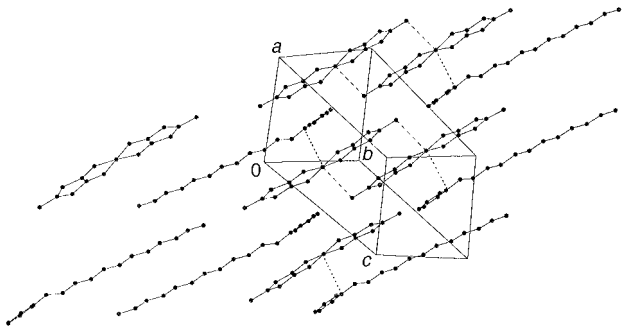

Fig. 15 Crystal structure of **2**, showing short inter-ion contacts

didecyldimethylammonium–Pd(dmit)$_2$. Roberts *et al.*[19] have shown that identical activation energies for Ohmic and SCL conduction is indicative of extrinsic behaviour with ΔE equal to the depth of the dominant trap.

Similar non-linear behaviour was observed in the plots of $\log_e$(current) *versus* reciprocal temperature for data obtained from conductive films of complex **1** that were deposited from floating films formed under different spreading conditions. The values of ΔE and α that were measured are collated in Table 2. In all cases (as-deposited and iodine-doped) the conductivity was thermally activated, with an activation energy of 0.07 ± 0.02 eV. This value is similar to that observed for films of C_{18}Py–Ni(dmit)$_2$ after exposure to iodine. There was also a power law variation of conductivity for complex **1** with temperature, $\sigma \propto T^{\alpha}$, where α was dependent on the spreading time and doping state, and lay in the range $1.4 \leqslant \alpha \leqslant 4.0$. A value of $\alpha = 1.5$ can be attributed to the temperature dependence of the density of states in the transport band, and larger values to a combination of this effect with a contribution due to a variation of mobility with temperature.

X-Ray crystal structure of complex 2

Single crystals of complex **1** could not be obtained. However, the dodecylpyridinium analogue **2** afforded dark green crystals which were suitable for X-ray analysis. The structure of **2** consists of separate $[Pd(dmit)_2]^-$ anions and $C_5H_5N^+(CH_2)_{11}Me$ cations (Fig. 15). In the anion, the Pd atom has a slightly (± 0.04 Å) distorted square planar coordination. Essentially planar dmit ligands form a dihedral angle of 5.6° at the Pd atom. The side chain of the cation adopts an almost ideal *trans*-planar conformation with all torsion angles within the range 175.0–178.4°. Its mean plane and that of the pyridine ring form a dihedral angle of 21.8°, and angles of 17.0 and 14.6°, respectively, with the mean plane of the anion.

To the best of our knowledge, this is the first structural study of a $[Pd(dmit)_2]^-$ *mono*anion. The structures studied so far contain either a dianion, in $(Bu_4N)_2[Pd(dmit)_2]$ **3**,[28] or formally hemianionic moiety in $A[Pd(dmit)_2]_2$ compounds **4** (A = Me_4N, Me_4As, Me_4P and Cs),[29] or 1:1 complexes with partial charge transfer in (BEDT-TTF)[Pd(dmit)$_2$] (**5**).[30] However, the geometry of dmit ligands and the Pd–S distances (average of 2.287 Å in **2**, *cf.* 2.314 in **3**, 2.293–2.298 in **4**, and 2.287 Å in **5**) show no systematic dependence on the formal charge on the Pd(dmit)$_2$ unit.

The structure of **4** contains segregated stacks of cations and anions, the latter consisting of dimers with Pd···Pd distances of 3.12–3.17 Å. No such stacks exist in the structure of **2**, where anions pack in centrosymmetric dimers with the interplanar separation of *ca.* 3.5 Å and Pd···S(5′) contacts of 3.57 Å, separated by cations (with a Pd···N contact of 3.83 Å). The shortest S···S contacts in the structure of **2** are between inversion-related anions contacting in a parallel edge-to-edge manner, *viz.* S(2)···S(2′) 3.44, S(2)···S(7′) 3.75 and S(4)···S(7′) 3.52 Å (Fig. 16) but those do not give rise to any continuous chain.

Conclusions

We have described the preparation and characterisation of LB films of (*N*-octadecylpyridinium)–Pd(dmit)$_2$ (complex **1**). The amount of material applied to the subphase and the length of time that this material was allowed to age on the surface of the subphase before compression and dipping were found to be critical in determining the properties of the floating layers. The material spread out well to give a large area per complex

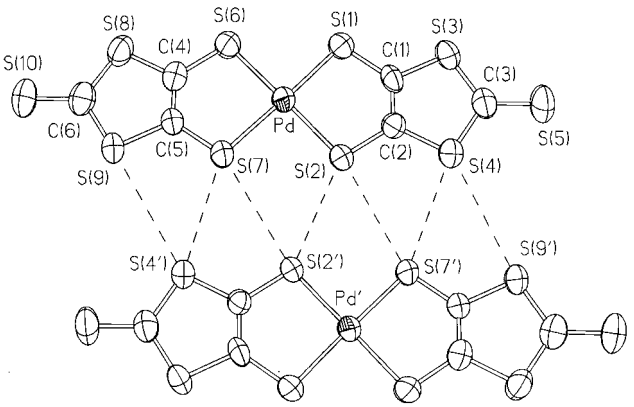

Fig. 16 $[Pd(dmit)_2]^-$ anions in the structure of **2**, showing thermal ellipsoids (at 50% probablility level) and S···S contacts

Table 2 Room temperature, in-plane conductivities together with thermal activation energies and values of α to give good straight line fits to the experimental data obtained from low temperature measurements on samples of complex **1** that were prepared under different experimental conditions

amount of solution spread/ml	spreading time	doping state	room temperature conductivity/S cm^{-1}	applied bias/V	ΔE ± 0.01 eV	α
1	10 min	as-deposited	$3.5 \pm 2.5 \times 10^{-3}$	1	0.07	4.0
				200	0.05	3.4
		iodine doped	$2.6 \pm 1.7 \times 10^{-2}$	1	0.09	1.4
1	18 h	as-deposited	$< 10^{-8}$		—	
		iodine doped	$< 10^{-8}$		—	
2	10 min	as-deposited	$1.5 \pm 1.0 \times 10^{-1}$	1	0.07	1.4
		iodine doped	$6.0 \pm 4.0 \times 10^{-2}$	1	0.06	2.5
2	21 h	as-deposited bulk	$< 10^{-8}$		—	
		iodine doped	$< 10^{-8}$		—	
		as-deposited aggregate	$1.2 \pm 1.0 \times 10^{-1}$	1	0.06	1.5
		iodine doped	$4.0 \pm 3.3 \times 10^{-2}$	1	0.06	2.1

value only if a small amount of material was used and a long time allowed before an isotherm was recorded. These poor spreading characteristics were reflected in the properties of multilayer films after transfer to a glass substrate. As with $C_{18}Py$–Ni(dmit)$_2$, thin layers, suggesting monolayer behaviour, were only observed if the amount of spreading solution applied to the subphase was small and a long time allowed before compression and transfer of the floating film. In contrast to multilayer LB films of $C_{18}Py$–Ni(dmit)$_2$, high bulk conductivity that was stable with time was observed without any post deposition treatment, but only if the floating film was compressed soon after spreading. It is thought that these films contained conductive crystallites, and that, with time, a reorganisation occurred to give an ordered monolayer structure in which the (dmit)$_2$ moieties were separated from each other and carrier transport was not favoured. Langmuir–Blodgett films of complex **1** deposited from a large amount of material that had been aged for many hours before compression contained large conductive aggregates. These formed on the surface of the subphase and were subsequently transferred to the substrate. In films deposited from a floating layer formed from a small amount of solution that was compressed soon after application to the surface of the subphase, a super-Ohmic dependence of current on bias voltage was observed. By observing the dependence of sample current in the super-Ohmic regime on the distance between contacts, this behaviour has been attributed to single carrier space-charge-limited conductivity. Observation of the low temperature electrical behaviour of conductive films of complex **1** has revealed semiconducting behaviour with a thermal activation energy for conductivity of 0.07 ± 0.02 eV, a value comparable to that obtained from LB layers of $C_{18}Py$–Ni(dmit)$_2$ after doping, *i.e.* 0.05 ± 0.01 eV. Plots of $\log_e$(current) *versus* reciprocal temperature were not perfect straight lines, however, indicating that there was also a power law variation of conductivity with temperature. This suggests a contribution to the temperature dependence of the conductivity from fluctuations in the density of states in the transport band and/or the carrier mobility. The single crystal X-ray structure of the analogous complex **2** provides the first structural study of a $[Pd(dmit)_2]^-$ *mono*anion.

We thank the UK Engineering and Physical Sciences Research Council (EPSRC) for their financial support.

References

1 Reviews: (*a*) M. R. Bryce and M. C. Petty, *Nature*, 1995, **374**, 771; (*b*) T. Nakamura, in *Handbook of Organic Conductive Molecules and Polymers*, ed. H. S. Nalwa. Wiley, Chichester, 1997, vol. 1, p. 727.

2 (*a*) A. Ruaudel-Teixier, M. Vandevyver and A. Barraud, *Mol. Cryst. Liq. Cryst*., 1985, **120**, 319; (*b*) T. Nakamura, M. Tanaka, T. Sekiguchi and Y. Kawabata, *J. Am. Chem. Soc*., 1986, **108**, 1302; (*c*) J. Richard, M. Vandevyver, P. Lesieur, A. Ruaudel-Teixier and A. Barraud, *J. Chem. Phys*., 1987, **86**, 2428.

3 (*a*) A. S. Dhindsa, M. R. Bryce, J. P. Lloyd and M. C. Petty, *Thin Solid Films*, 1988, **165**, L97; (*b*) A. S. Dhindsa, J. P. Badyal, M. R. Bryce, M. C. Petty, A. J. Moore and Y. M. Lvov, *J. Chem. Soc., Chem. Commun*., 1990, 970; (*c*) A. S. Dhindsa, Y-P. Song, J. P. Badyal, M. R. Bryce, Y. M. Lvov, M. C. Petty and J. Yarwood, *Chem. Mater*., 1992, **4**, 724; (*d*) G. Cooke, A. S. Dhindsa, Y. P. Song, G. Williams, A. S. Batsanov, M. R. Bryce, J. A. K. Howard, M. C. Petty and J. Yarwood, *Synth. Met*., 1993, **55–57**, 3871.

4 For recent work on LB films of nonamphiphilic TTF derivatives see: L. M. Goldenberg, J. Y. Becker, O. P.-T. Levi, V. Y. Khodorkovsky, L. M. Shapiro, M. R. Bryce, J. P. Cresswell and M. C. Petty, *J. Mater. Chem*., 1997, **7**, 901.

5 (*a*) P. Cassoux and L. Valade, in *Inorganic Materials*, ed. D. W. Bruce and D. O'Hare, Wiley, Chichester, 1992, pp. 1–58; (*b*) A. Kobayashi, A. Sato, K. Kawano, T. Naito, H. Kobayashi and T. Watanabe, *J. Mater. Chem*., 1995, **5**, 1671; (*c*) A. E. Pullen, H-L. Liu, D. B. Tanner, K. A. Abboud and J. R. Reynolds, *J. Mater. Chem*., 1997, **7**, 377.

6 T. Nakamura, K. Kojima, M. Matsumoto, H. Tachibana, M. Tanaka, E. Manda and Y. Kawabata, *Chem. Lett*., 1989, 367.

7 D. M. Taylor, S. K. Gupta, A. E. Underhill and A. S. Dhindsa, *Thin Solid Films*, 1994, **243**, 530.

8 (*a*) A. S. Dhindsa, J. P. Badyal, C. Pearson, M. R. Bryce and M. C. Petty, *J. Chem. Soc., Chem. Commun*., 1991, 322; (*b*) C. Pearson, A. S. Dhindsa, M. C. Petty and M. R. Bryce, *Thin Solid Films*, 1992, **210/211**, 257.

9 (*a*) C. Pearson, A. J. Moore, J. E. Gibson, M. R. Bryce and M. C. Petty, *Thin Solid Films*, 1994, **244**, 932; (*b*) C. Pearson, J. E. Gibson, A. J. Moore, M. R. Bryce and M. C. Petty, *Electron. Lett*., 1993, **29**, 1377.

10 G. Williams, A. J. Moore, M. R. Bryce and M. C. Petty, *Thin Solid Films*, 1994, **244**, 936.

11 C. Pearson, A. S. Dhindsa, L. M. Goldenberg, R. A. Singh, R. Dieing, A. J. Moore, M. R. Bryce and M. C. Petty, *J. Mater. Chem*., 1995, **5**, 1601.

12 N. W. Alcock and P. J. Marks, *J. Appl. Crystallogr*., 1994, **26**, 200.

13 G. M. Sheldrick, *Acta Crystallogr., Sect. A*, 1990, **46**, 467.

14 G. M. Sheldrick, SHELXL-93, Program for the refinement of crystal structures, University of Göttingen, Germany, 1993.

15 M. C. Petty, *Langmuir–Blodgett films: an introduction*, Cambridge University Press, Cambridge, 1996.

16 D. M Taylor, A. E. Underhill, S. K. Gupta and C. E. Wainwright, *Makromol. Chem., Makromol. Symp*., 1991, **46**, 199.

17 (*a*) S. K. Gupta, D. M. Taylor, P. Dynarowicz, E. Barlow, C. E. A. Wainwright and A. E. Underhill, *Langmuir*, 1992, **8**, 3057; (*b*) S. K. Gupta, D. M. Taylor, A. E. Underhill and C. E. A. Wainwright, *Synth. Met*., 1993, **58**, 373.

18 M. Yumura, T. Nakamura, M. Matsumoto, S. Ohshima, Y. Kuriki, K. Honda, M. Kurahashi and Y.F. Miura, *Synth. Met*., 1993, **55–57**, 3865.

19 A. E. Underhill, R. A. Clark, I. Marsden, M. Allan, R. H. Friend, H. Tajima, T. Naito, M. Tamura, H. Kuroda, A. Kobayashi, H. Kobayashi, E. Canadell. S. Ravy and J. P. Pouget, *J. Phys.: Condens. Matter*, 1991, **3**, 933.

20 Y. F. Miura, M. Takenaga, A. Kasai, T. Nakamura, M. Matsumoto and Y. Kawabata, *Jpn. J. Appl. Phys*., 1991, **30**, 3503.

21 R. J. Ward, A. S. Dhindsa, M. R. Bryce, M. C. Petty and H. S. Munro, *Thin Solid Films*, 1991, **198**, 363.

22 G. G. Roberts, N. Apsley and R. W. Munn, *Physics Rep*., 1980, **60**, 61.

23 G. G. Roberts in *Transfer and Storage of Energy by Molecules*, ed. A. M. North, G. M. Burnet and J. N. Sherwood, Wiley, Chichester, 1974, p. 163.

24 D. M. Taylor, S. K. Gupta, A. E. Underhill and C. E. A. Wainwright, *Thin Solid Films*, 1992, **210/211**, 287.

25 A. J. Epstein, E. M. Conwell and J. S. Miller, *Ann. N. Y. Acad. Sci*., 1978, 183.

26 T. Nakamura, H. Tanaka, M. Matsumoto, H. Tachibana, E. Manda and Y. Kawabata, *Synth. Met*., 1988, **27**, B601.

27 Y. F. Miura, M. Takenaga, A. Kasai, T. Nakamura, Y. Nishio, M. Matsumoto and Y. Kawabata, *Thin Solid Films*, 1992, **201/211**, 306.

28 Qian Minxie, Zhu Naijue and Zhu Daoben, *Jiegou Huaxue (J. Struct. Chem.)*, 1985, **4**, 86.

29 (*a*) A. Kobayashi, H. Kim, Y. Sasaki, K. Murata, R. Kato and H. Kobayashi, *J. Chem. Soc., Faraday Trans*., 1990, **86**, 361; (*b*) C. Faulmann, J.-P. Legros, P. Cassoux, J. Cornelissen, L. Brossard, M. Inokuchi, H. Tajima and M. Tokumoto, *J. Chem. Soc., Dalton Trans*., 1994, 249; (*c*) R. A. Clark and A. E. Underhill, *Synth. Metals*, 1988, 27, B515.

30 Qian Minxie, Fu Heng and Zhu Daoben, *Jiegou Huaxue (J. Struct. Chem.)*, 1986, 5, 127.

Paper 7/04579D; *Received* 30*th June*, 1997